

A Study of Beam-Pattern Generation Methods for Antenna Array Systems

WEI-CHIANG WU and YUAN-JIUN WANG

Department of Communication Engineering, Da-Yeh University

112 Shan-Jiau Rd., Da-Tsuan, Changhua, Taiwan

ABSTRACT

This report aims to provide a systematic study of several beam-pattern generation algorithms in an antenna array system. The weights are derived to best approximate a desired array pattern, either in a minimum-mean-square-error (MMSE) sense or to satisfy specific array pattern requirements. By sampling the specified (desired) spatial response at regular intervals, the first method performs a discrete Fourier transform (DFT) directly on the sampled sequence to derive the weights. The second method is premised on choosing appropriate window functions to attain the goals of sidelobe attenuation and steep transition from passband to stopband. Simulation results demonstrate that the generated beam pattern can be flexibly shaped, steered, and gain-controlled for practical requirements.

Key Words: beam pattern, weights, minimum-mean-square-error, discrete Fourier transform, sidelobe, transition

針對陣列天線系統之電波波束產生方法之研究

武維疆 王元鈞

大葉大學電信工程系

彰化縣大村鄉山腳路 112 號

摘要

本論文試圖針對陣列天線系統的波束產生演算法提供一個系統化的研究，在考慮最接近理想波束型態以及滿足最小平方誤差（MMSE）還有一些特殊的要求的情況下，天線的權值（weights）被推導出來，第一個演算法針對理想的空間響應在特定的區間內做取樣，並利用離散傅立葉（DFT）技術推導出天線的權值，第二個方法選擇適當的窗函數（window function）以達到旁波帶（sidelobes）衰減或過渡帶（transition）變陡。由模擬結果可推證其產生的合成波束可以有彈性地成為適當的形狀，並具有可調整性以及增益控制的特性更符合實際的需求。

關鍵詞：波束型態，陣列天線之天線權值，最小均方誤差，離散傅立葉轉換，窗函數，旁波帶，過渡帶

I. INTRODUCTION

As extensively analyzed in [1], the issues that adversely affect the capacity of a cellular network include unbalanced traffic load, handoff overhead, and pilot signals interference. It is desirable to generate any radiation pattern in time-varying, software controlled sense such that the problems can be mitigated. However, conventional sectorized cell can hardly change the beam width, shape and even redirect the sector orientation. Thanks for the smart antennas technology, any specific radiation pattern can be approximated by properly determining the excitation, that is, the weight of each antenna element.

Quite a few papers have been proposed to design the weight to minimize the mean-squared error (MSE) between the desired and the generated beam patterns [2-4]. It is evident that the optimum solution in a least-squares sense leads to the Wiener solution [5]. Additional constraints can also be included to the least-squares criterion in order to satisfy practical situation or specific sidelobe topography. As depicted in [2-4], there are main beam constraint (beamwidth steering), nulls constraints (null steering), equi-sidelobe levels and maximum sidelobe energy constraints. Main difficulties in applying the constraint optimization algorithm include:

1. The explicit function of the desired pattern is hard to obtain.
2. The integration of the squared-error function may be not easy to calculate.
3. The load of computation increases as we perform matrix inverse with large size.

In this paper, we develop two simple beam-pattern synthesis methods. The first algorithm exploits the well-known DFT and IDFT techniques [7], where the "frequency" is converted into the "spatial" domain. The desired radiation pattern (spatial response) is first equally-spaced sampled to obtain a discrete-space representation of the desired spatial response. Then, the excitation (weight) for each antenna element can be derived by performing DFT on the data sequence. Main benefit of the spatial spectrum sampling method is that it needs only the information of regular points of the desired pattern in spatial domain, not the entire function. Moreover, the fast Fourier transform (FFT) algorithm may be applied to extensively reduce the load of computations.

Rather than minimizing the MSE between the desired spatial response and the estimated one, the second method premises on the design criterion to meet specific "shape" requirement. In practical situation, the design criterion is the sidelobe level, and/or steepness of the transition from passband to stopband, and/or ripples. As described in [7], it is plausible

to apply a class of window functions for the design of finite-impulse-response (FIR) digital filter. While in this research, we fully exploit the windowing concept for beam pattern shaping. Both methods are simple in structure and can be efficiently applied in wireless communication.

II. SYSTEM MODLE

Throughout this paper, a uniform linear array (ULA) with array size $N=2M+1$ and antenna element spacing d is assumed. Without loss of generality, we use the center antenna element as reference point and the received pattern can thus be determined by [6]

$$P(\theta) = \sum_{n=-M}^M w_n \exp\left(j \frac{2\pi}{\lambda} nd \sin \theta\right) \quad (1)$$

where w_n accounts for the weight assigned to the n th antenna element. λ is the wavelength and θ is the direction of arrival (DOA) measured relative to the array normal. Note that the field of view (FOV) of an ULA is $180^\circ(-90^\circ \sim 90^\circ)$. We attempt to generate any desired pattern, or equivalently, spatial spectrum, by a set of appropriately chosen weights. To possess spatial information and avoid grating lobe problem, we choose $d = \frac{\lambda}{2}$. Let $x = -\pi \sin \theta$, we can convert (1) into a function of x

$$P(x) = \sum_{n=-M}^M w_n \exp(-jnx) \quad (2)$$

It is apparent that $P(x)$ is the weighted sum of a set of complex exponentials, $\{\exp(-jnx)\}_{n=-M, \dots, 0, \dots, M}$. The inner product of $\{\exp(-jnx)\}_{n=-M, \dots, 0, \dots, M}$ within $x \in [-\pi, +\pi]$ can be obtained as

$$\int_{-\pi}^{\pi} \exp(-jnx) \exp(jmx) dx = \begin{cases} 2\pi, m = n \\ 0, m \neq n \end{cases} \quad (3)$$

Equation (3) reveals that $\{\exp(-jnx)\}_{n=-M, \dots, 0, \dots, M}$ form an orthogonal set within $x \in [-\pi, +\pi]$. Hence, (2) corresponds to an orthogonal expansion of $P(x)$ by the basis functions $\{\exp(-jnx)\}_{n=-M, \dots, 0, \dots, M}$. By exploiting the orthogonality property of (3), the coefficients (weights) can be obtained:

$$w_n = \frac{1}{2\pi} \int_{-\pi}^{\pi} P(x) \exp(jnx) dx \quad n = -M, \dots, 0, \dots, M \quad (4)$$

Alternatively, if it is required to generate a desired spatial

spectrum $d(x)$, which is at least piecewise-continuous within the FOV of an ULA, then the mean square error (MSE) between $d(x)$ and the synthesized pattern, $P(x)$, can be defined as

$$e(N) \equiv \int_{-\pi}^{+\pi} \left| d(x) - \sum_{n=-M}^M w_n \exp(-jnx) \right|^2 dx \quad (5)$$

We attempt to find a set of weights, $\{w_n\}$, such that $e(N)$ is minimized. By differentiating $e(N)$ with respect to w_n and setting the result to zero, the optimum weight can be obtained as follows

$$w_n = \frac{1}{2\pi} \int_{-\pi}^{+\pi} d(x) \exp(jnx) dx \quad n = -M, \dots, 0, \dots, M \quad (6)$$

Comparing (6) with (4), it is evident that the optimum weights that minimize the MSE between the desired and generated pattern are equivalent to the coefficients of an orthogonal expansion. More specifically, substituting (6) into (5), we arrive at the minimized MSE:

$$e(N) = \int_{-\pi}^{+\pi} d^2(x) dx - 2 \sum_{n=-M}^M |w_n|^2 \quad (7)$$

Due to the fact that $|w_n|^2$ is nonnegative, $e(N)$ is a monotonically decreasing function with respect to N . In other words, the MSE between $d(x)$ and the synthesized pattern, $P(x)$, can be made arbitrary small as we increase the array size.

$$\lim_{N \rightarrow \infty} e(N) = 0 \quad (8)$$

It should be noted that (2) and (4) is the counterpart of discrete-time Fourier transform (DTFT) and inverse discrete-time Fourier transform (IDTFT), respectively. We refer them as discrete space Fourier transform (DSFT) pairs since they are utilized to synthesize desired spatial spectrum rather than frequency spectrum. From (5)~(8), it is evident that the Fourier transform design method gives the optimum solution in a least-squares sense.

III. BEAM PATTERN GENERATION METHODS

We start with a desired spatial spectrum as shown in Fig. 1, where the region $x \in [-x_1, +x_1]$ is distortionlessly passed and the region other than $x \in [-x_1, +x_1]$ should be completely suppressed. Based on the IDSFT method, the required weights

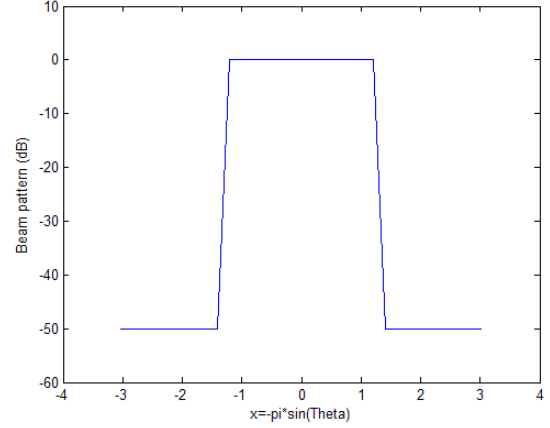


Fig. 1. Ideal “low-pass” spatial spectrum

can be calculated from (4):

$$\begin{aligned} w_n &= \frac{1}{2\pi} \int_{-\pi}^{+\pi} P(x) \exp(jnx) dx = \frac{1}{2\pi} \int_{-x_1}^{x_1} 1 \cdot \exp(jnx) dx \\ &= \frac{1}{n\pi} \sin(nx_1) \\ &= \frac{x_1}{\pi} \text{sinc}(nx_1) \end{aligned} \quad (9)$$

where $\text{sinc}(x) = \sin(x)/x$. The approach is conceptually straightforward, but there are two difficulties in practical realization:

- The integration of $\int_{-\pi}^{+\pi} P(x) \exp(jnx) dx$ is not always solvable.
- The number of weights needed to generate $P(x)$ is usually prohibitively large, giving rise to an impractical array size. As indicated by (9), the sinc function leads to infinite number of terms.

1. Spatial Spectrum Sampling Method

It is easy to show that (2) is a periodic function of x with period 2π , $P(x) = P(x + 2k\pi)$. Sampling $P(x)$ at $N = 2M + 1$ equally-spaced points within one period, thus eq. (2) can be rewritten as discrete form:

$$P(x_k) = \sum_{n=-M}^M w_n \exp\left(-j \frac{2n\pi k}{N}\right); k = -M, \dots, 0, \dots, M \quad (10)$$

where $x_k = \frac{2\pi k}{N}$. With regard to (3), the basis functions in

discrete form still possess the orthogonality characteristics

$$\sum_{n=-M}^M \exp\left(-j \frac{2n\pi k}{N}\right) \exp\left(+j \frac{2m\pi k}{N}\right) = N \delta(n - m) \quad (11)$$

The corresponding weights in (10) can be obtained as

$$w_n = \frac{1}{N} \sum_{k=-M}^M P(x_k) \exp\left(j \frac{2n\pi k}{N}\right); n = -M, \dots, 0, \dots, M \quad (12)$$

It is apparent from (12) that the number of weights derived from the spatial spectrum sampling method is finite. And the integration operation as depicted in (4) is replaced by summation. Moreover, the spatial spectrum sampling method requires only N points of the desired spatial pattern, not the continuous function, $d(x)$. The design process is summarized as follows:

Step 1: Specify the desired ideal spatial response

Step 2: Sample the desired spatial response at regular intervals along the spatial domain, to obtain the uniformly-spaced representation.

Step 3: Exploit (12) and the data sequence obtained in Step 2 to derive the weights $w_{n,DFT}$.

Step 4: Obtain the resultant spatial spectrum by substituting $w_{n,DFT}$ into the DSFT equation:

$$P(x) = \sum_{n=-M}^M w_{n,DFT} \exp(-jnx) \quad (13)$$

2. Windowing Method

As described in (9), the IDSFT leads to the weight with infinite number of terms that is physically unrealizable. Truncating w_n is equivalent to multiplying the ideal solution w_n by a finite-length window function h_n . Several window functions that are widely applied in the design of FIR (nonrecursive) digital filter can be utilized for weight design. Rather than the minimization of MSE, the design criteria are the sidelobe level and the steepness of the transition from passband to stopband. The low-pass spatial filter design steps for windowing method can be categorized as follows:

Step 1: Determine the ‘‘cutoff’’ angle, x_1 , of the desired spatial spectrum. As a rule of thumb [7], it can be calculated by:

$$\text{cutoff angle} = \text{passband edge angle} + \frac{\text{transition width}}{2}$$

Step 2: Calculate the ideal weights:

$$w_n = \frac{1}{n\pi} \sin(nx_1) \quad (14)$$

Step 3: Choose an appropriate window that will satisfy the requirement of sidelobe attenuation.

Step 4: Determine the window length to meet the specification of the desired transition width (steepness of the spatial

filter)

Step 5: Calculate the composite weights by multiplying w_n by a finite-length window function h_n :

$$\tilde{w}_{n,LP} = w_n h_n \quad (15)$$

Step 6: Obtain the resultant spatial spectrum by substituting $\tilde{w}_{n,LP}$ into the DSFT equation.

Intuitively, the steeper the required roll-off of the filter, the larger the number of terms (window length) is needed.

The band-pass or high-pass spatial filter can be derived based on the low-pass prototype. In what follows, the desired band-pass or high-pass spatial spectrum is first shifted down to the low-pass prototype. Then the design step is similar to the low-pass spatial filter except that $\tilde{w}_{n,LP} = w_n h_n$ in Step 5 should be modified for band-pass filter as

$$\tilde{w}_{n,BP} = w_n h_n \cos(nx_0) \quad (16)$$

where x_0 is the center angle of the band-pass filter. Similarly, $\tilde{w}_{n,LP} = w_n h_n$ should be modified for high-pass filter as

$$\tilde{w}_{n,HP} = w_n h_n \cos(n\pi) \quad (17)$$

Note that both (16) and (17) are direct applications of the modulation property of Fourier transform.

If it is required to generate a bandstop (or notch) spatial spectrum for rejecting a band of unwanted arriving angles, a combination of the above techniques can attain the goal. The obvious approach is to design a low-pass and a high-pass spatial filter with the cutoff angles set to be the lower end and higher end of the stopband angles, respectively. The low-pass and high-pass spatial filters are placed in parallel. Consequently, the equivalent composite weights can be obtained as

$$\tilde{w}_{n,BS} = \tilde{w}_{n,HP} + \tilde{w}_{n,LP} \quad (18)$$

IV. SIMULATION EXAMPLES

In this section, we will conduct some numerical examples to evaluate the performance of the methods described in Sec. 3. We start with the design of a low-pass spatial filter with cutoff angle $x_1 = \frac{\pi}{3} = 1.0472$. In other words, by appropriately choosing weights, the array should pass source signals with bearings $x \in \left[-\frac{\pi}{3}, +\frac{\pi}{3}\right] = [-1.0472, 1.0472]$ while

suppress signals with DOAs other than $x \in \left[-\frac{\pi}{3}, +\frac{\pi}{3}\right] = [-1.0472, 1.0472]$. The spatial spectrum sampling method with $N=31$ is first performed following the steps described in Sec. 3.1. The generated low-pass spatial spectrum is shown in Fig. 2. (a) with sample size $N=31$ points sampled from ideal “low-pass” spatial spectrum Fig.1., (b) with sample size $N=91$ points sampled from ideal “low-pass” spatial spectrum Fig.1.). We then demonstrate the windowing method as depicted in Sec. 3.2 and present the result in Fig. 3. Note that *Hamming window* with window function [7]

$$h_n = 0.54 + 0.46 \cos\left(\frac{2\pi n}{N-1}\right) \quad (19)$$

and window length $N=31$ are chosen for the simulation. to generate the pattern in Fig. 3. (where the cutoff angle is $x_1 = \frac{\pi}{3} = 1.0472$). As the window length or array size, N , increases to 91, we present the resultant beam pattern in Fig. 4.

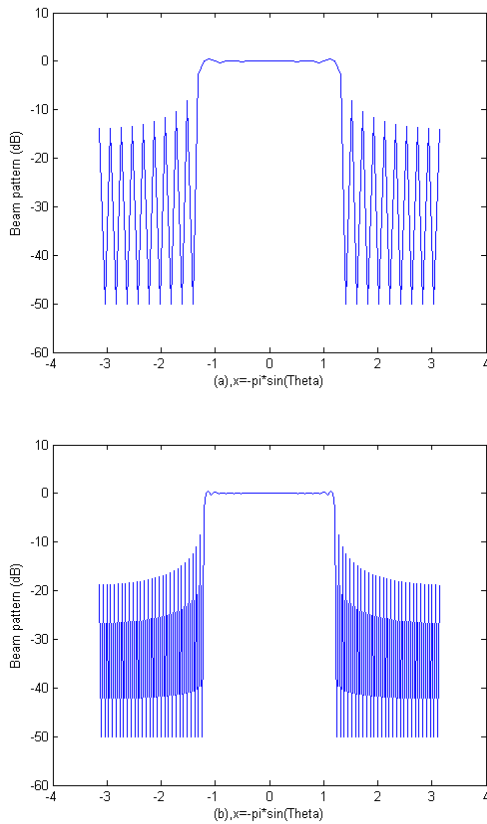


Fig. 2. Using spatial spectrum sampling method to generate a “low-pass” pattern

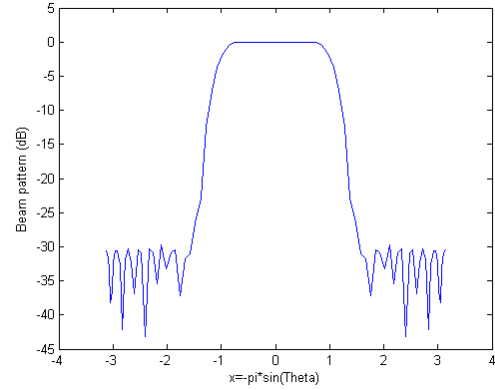


Fig. 3. Using windowing method to generate a low-pass spatial spectrum (window length $N=31$)

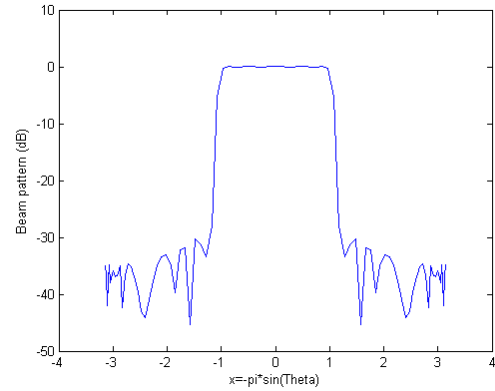


Fig. 4. Using windowing method to generate a low-pass spatial spectrum (window length $N=91$)

As revealed in Fig. 4, it is more approximate to the desired pattern especially for the reduction of transition width. Moreover, as we compare Fig. 3 with Fig. 4, it is clearly shown that the sidelobe level has been reduced at the expense of larger array size.

The second example aims to verify the design of high-pass spatial filter. In contrast to low-pass spatial filter, the design criterion is to suppress signals originating from the bearings $x \in [-x_1, +x_1]$, with $0 \leq x_1 \leq \pi$. In this simulation, we set the desired specifications for the high-pass spatial filter as follows:

- A. pass-band edge at $\theta=70^\circ$ ($x_1=1.2217$, $x \in [-1.2217, 1.2217]$)
- B. stop-band attenuation at least 50dB
- C. transition width = 20°

Following the design steps in section 3, we derive the weights and generate the corresponding beam pattern in Fig. 5. As shown in Fig. 5, the spectrum matches the desired specifications except for slight sidelobes and ripples.

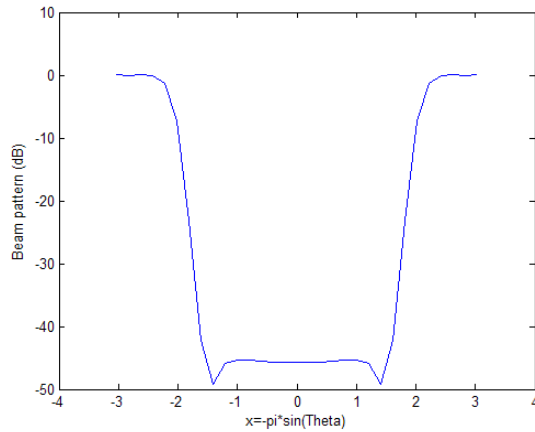


Fig. 5. Using windowing method to generate a high-pass spatial spectrum (window length $N=31$)

A bandstop spatial filter is designed in the final example. The goal is to reject or notch signals around a specific angle. The desired specifications are attached as follows:

A. stop band $\theta = 15^\circ \sim 40^\circ$, ($x=0.2618 \sim 0.6981$ and $-0.6681 \sim -0.2618$)

B. transition width = 10°

Exploiting *Hamming window* with length $N=31$ for the design of both the low-pass and high-pass spatial filters, we can utilize (18) to obtain the composite weights, $\tilde{w}_{n,BS} = \tilde{w}_{n,HP} + \tilde{w}_{n,LP}$.

As shown in Fig. 6, the generated spatial spectrum satisfies the desired specifications.

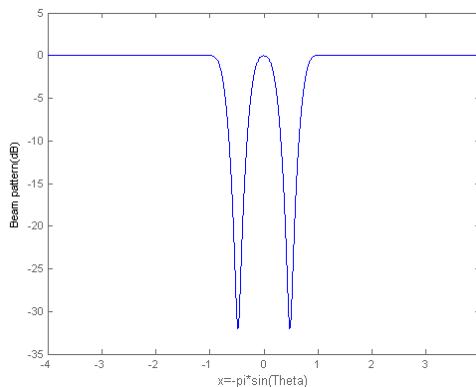


Fig. 6. Using windowing method to generate a band-stop spatial spectrum (window length $N=31$)

V. CONCLUSIONS

In this paper, two flexible array beam pattern generation methods have been proposed. The spatial spectrum sampling method is based on the DFT and IDFT rationale. The resultant spatial spectrum approximates the desired one in MMSE sense. The windowing method premises on satisfying specific pattern topology. A class of window functions are appropriately chosen to truncate the ideal weights. We have demonstrated from the simulation examples that the array pattern including main beam width and shapes, sidelobe topology can be generated to approximate the desired radiation pattern.

REFERENCES

1. Gordon, S. D. (2000) *Smart Cell Site Optimization CDMA Solutions Seminar Series*, seminar two. Metawave Communication Corporation, Washington, USA.
2. Nagesh S. R. and T. S. Vedavathy (1995) A procedure for synthesizing a specified sidelobe topography using an arbitrary array. *IEEE Transactions on Antennas and Propagation*, 43(7), 742-745.
3. Ng, B. P., M. H. Er and C. Kot (1993) A flexible array synthesis method using quadratic programming. *IEEE Transactions on Antennas and Propagation*, 41(11), 1541-1550.
4. Tseng, C. Y. and L. J. Griffiths (1992) A simple algorithm to achieve desired patterns for arbitrary arrays. *IEEE Transactions on Antennas and Propagation*, 40(11), 2737-2746.
5. Haykin, S. (2002) *Adaptive Filter Theory*, 94-107. Prentice Hall, Upper saddle River, NJ.
6. Van Trees, H. L. (2002) *Optimum Array Processing*, 90-200. John Wiley & Sons, Inc., New York, NY.
7. Vegte Joice, Van de (2002) *Fundamentals of Digital Signal Processing*, 315-373. Prentice Hall, Upper saddle River, NJ.

收件：93.02.17 修正：93.05.04 接受：93.07.03